



Matrix metalloproteinase 14 regulates HSV-1 infection in neuroblastoma cells

Patricia Llorente^{a,b}, Víctor Mejías^a, Isabel Sastre^{a,b}, María Recuero^{a,b,c}, Jesús Aldudo^{a,b,c,**},
 Maria J. Bullido^{a,b,c,*}

^a Centro de Biología Molecular “Severo Ochoa” (C.S.I.C.-U.A.M.), Universidad Autónoma de Madrid, C/ Nicolás Cabrera 1, 28049, Madrid, Spain

^b Centro de Investigación Biomédica en Red Sobre Enfermedades Neurodegenerativas, (CIBERNED), Madrid, Spain

^c Instituto de Investigación Sanitaria “Hospital La Paz” (IdIPaz), Madrid, Spain

ARTICLE INFO

Keywords:

Herpes simplex virus type 1
 Matrix metalloproteinase 14
 Neurodegeneration
 Alzheimer's disease
 Antiviral target

ABSTRACT

Growing evidence supports that chronic or latent infection of the central nervous system might be implicated in Alzheimer's disease (AD). Among them, Herpes simplex virus type 1 (HSV-1) has emerged as a major factor in the etiology of the disease. Our group is devoted to the study of the relationship among HSV-1, oxidative stress (OS) and neurodegeneration. We have found that HSV-1 induces the main neuropathological hallmarks of AD, including the accumulation of intracellular amyloid beta (A β), hyperphosphorylated tau protein and autophagic vesicles, that OS exacerbates these effects, and that matrix metalloproteinase 14 (MMP-14) participates in the alterations induced by OS.

In this work, we focused on the role of MMP-14 in the degenerative markers raised by HSV-1 infection. Interestingly, we found that MMP-14 blockage is a potent inhibitor of HSV-1 infection efficiency, that also reduces the degeneration markers, accumulation of A β and hyperphosphorylated tau, induced by the virus. Our results point to MMP-14 as a potent antiviral target to control HSV-1 infection and its associated neurodegenerative effects.

1. Introduction

1.1. Infectious hypothesis. Herpes simplex virus 1 in Alzheimer's disease

Growing evidence indicates that chronic or latent infection of the central nervous system might be implicated in the etiology of Alzheimer's disease (AD) (see recent reviews (Fulop et al., 2018; Haas and Lathe 2018; Harris and Harris 2015; Itzhaki 2016)). The idea of the so-called infectious hypothesis came up in the 1960s and has gained support especially in recent years (Harris and Harris, 2015, 2018). The hypothesis states that in combination with genetic risk factors, these pathogens participate in the accumulation of the amyloid β (A β) peptide, tau hyperphosphorylation and inflammation. Numerous findings support the involvement of neurotropic viruses from the *Herpesviridae* family, especially HSV-1, in AD pathogenesis (Eimer et al., 2018; Harris and Harris, 2018; Itzhaki 2016, 2018). Brain autopsies showed that latent HSV-1 is present in a high proportion of sporadic AD and normal

elderly individuals, and it was found in the areas most affected by AD, namely temporal and frontal cortices and hippocampus (Jamieson et al., 1991). Furthermore, the viral DNA seems to colocalize with senile plaques suggesting an active role of the virus in their generation (Wozniak et al. 2009). Evidence from epidemiological studies postulate that, in synergy with the possession of the APOE- ϵ 4 allele, HSV-1 infection represents a risk factor for AD (Itzhaki et al., 1997). Moreover, the presence of IgM anti-HSV antibodies in serum—a marker of recent HSV reactivation—was highly correlated with the progression of the disease (Letenneur et al., 2008); (Lovheim et al., 2015). On the other hand, HSV-1 has been linked to the main neuropathological hallmarks of AD in cellular and animal models of HSV-1 infection: accumulation of intracellular A β (Santana et al., 2012a, b; Wozniak et al., 2007), hyperphosphorylated tau protein (Alvarez et al., 2012; Wozniak et al. 2009) and autophagic vesicles (Itzhaki et al. 2008; Santana et al., 2012a, b). Our group has been studying the relationships among oxidative stress (OS), HSV-1 and neurodegeneration for several years. We showed that

* Corresponding author. Centro de Biología Molecular “Severo Ochoa”, Universidad Autónoma de Madrid, C/ Nicolás Cabrera 1, 28049, Madrid, Spain.

** Corresponding author. Centro de Biología Molecular “Severo Ochoa”, Universidad Autónoma de Madrid, C/ Nicolás Cabrera 1, 28049, Madrid, Spain.

E-mail addresses: pllorente@cbm.csic.es (P. Llorente), vmejias@cbm.csic.es (V. Mejías), isastre@cbm.csic.es (I. Sastre), mrecuero@cbm.csic.es (M. Recuero), jaldudo@cbm.csic.es (J. Aldudo), mariajesus.bullido@uam.es (M.J. Bullido).

<https://doi.org/10.1016/j.antiviral.2021.105116>

Received 12 April 2021; Received in revised form 2 June 2021; Accepted 3 June 2021

Available online 6 June 2021

0166-3542/© 2021 The Authors. Published by Elsevier B.V. This is an open access article under the CC BY license (<http://creativecommons.org/licenses/by/4.0/>).

Table 1
Primary antibodies.

Antigen	Clonality	Host	Dilution		Reference
			WB	IF	
gC	monoclonal	mouse	1:3000	1:500	Abcam (ab6509)
HSV-1	polyclonal	rabbit	–	1:500	Dako (B0114)
ICP4	monoclonal	mouse	1:1000	1:200	Abcam (ab6514)
A β 40	polyclonal	rabbit	–	1:100	Thermo Fisher (44344)
A β 42	polyclonal	rabbit	–	1:100	Thermo Fisher (44348A)
Tau-5	monoclonal	mouse	1:500	1:50	Thermo Fisher (AHB0042)
P-Tau (Thr205)	polyclonal	rabbit	–	1:100	ThermoFisher (44-738G)
P-Tau (Thr231)	polyclonal	rabbit	1:1000	–	ThermoFisher (44-746G)
Tubulin	monoclonal	mouse	1:10000	–	Sigma (T5168)

OS enhances the intracellular accumulation of A β induced by HSV-1 infection, and further decreased its secretion to the extracellular medium. OS also potentiated the accumulation of immature autophagic compartments and the inhibition of the autophagic flux induced by HSV-1. At the same time, OS reduced the efficiency of HSV-1 infection (Santana et al., 2013). Moreover, functional genomic analysis of our cell model of infection and OS revealed the lysosome system to be impaired, suggesting that the interaction of OS with HSV-1 affects lysosomal function (Kristen et al., 2018).

Recently, several reports have provided strong evidence of the implication of HSV-1 in AD pathogenesis. Multiscale analysis integrating genomic, transcriptomic, proteomic, and histopathological data provide compelling evidence that several herpesviruses (HSV-1; HHV-6A and HHV-7) contribute to the development of neuropathology and AD (Readhead et al., 2018). Moreover, A β binding to HSV-1 and HHV-6 surface causes fibrillar A β agglutination that can protect against viral challenge, suggesting that A β can be part of the innate immune response to infections (Eimer et al., 2018). Finally, a big epidemiological survey in the Taiwanese population raised the striking observation that the risk of senile dementia was much greater in HSV-seropositive subjects and that antiviral treatment caused a dramatic decrease in the development of dementia (Tzeng et al., 2018). These findings have refueled the field leading some researchers to claim for a change in the current paradigms relating the causes and mechanisms of AD (Fulop et al., 2018; Haas and Lathe 2018).

1.2. Role of MMPs in viral infections

The matrix metalloproteinase family (MMPs) belongs to the met-zincin group of proteases, which share a conserved zinc-binding motif in their active site. Recent data illustrate an extremely wide range of substrates and interconnections for these enzymes, locating them at the crossroads of many biological processes (Jobin et al. 2017; Young et al., 2019). Among them, MMP-14 (also known as MT1-MMP) is highly expressed in brain regions that show amyloid pathology and neuroinflammation.

MMPs have been shown to be involved in several viral infections. Excess MMP activity following infection may lead to immunopathology that causes host morbidity or mortality and favors pathogen dissemination or persistence (Elkington, O'Kane, and Friedland 2005). MMP-14 contributed to Influenza-related tissue damage and mortality, and its selective inhibition protected the tissue from infection-related structural and compositional tissue damage (Talmi-Frank et al., 2016). Deficiency of MMP-9, a gelatinase activated by MMP-14, diminished influenza A infection effects in mice, lowering lung viral titers and injury, weight loss and mortality rates (Rojas-Quintero et al., 2018). Moreover, the increase of MMP-9 expression is involved in the evolution of herpes simplex encephalitis by facilitating the development of cerebrovascular

complications (Martinez-Torres et al., 2004). Finally, HIV-induced MMP-9 activation promotes HSV-1 cell-to-cell spread in oral epithelial cells (Sufiawati and Tugizov 2018). Taking this relation among MMPs and viral infections into account, we decided to explore the role of MMP-14 in HSV-1 infection and the AD-like phenotype in cell models of neurodegeneration induced by the virus (Santana et al., 2012a, b, 2013).

2. Materials & methods

2.1. Cell lines

The SK-N-MC cells derived from human neuroepithelioma (HTB-10) were obtained from the American Type Culture Collection. These were cultured as a monolayer in minimal Eagle's medium supplemented with 10% heat-inactivated foetal calf serum, 1 mM sodium pyruvate, non-essential amino acids, 2 mM glutamine, and 50 μ g/mL gentamycin, at 37 °C in a humidified 5% CO₂ atmosphere. The murine neuroblastoma N2a cell line, kindly provided by P. Saftig, was cultured in Dulbecco's modified Eagle's medium supplemented with 10% heat-inactivated foetal calf serum, 1 mM sodium pyruvate, non-essential amino acids, 2 mM glutamine, and 50 μ g/mL gentamycin, at 37 °C in a humidified 5% CO₂ atmosphere.

MMP-14 deficient cells. The knockdown of MMP-14 was performed by transfection of SK-N-MC cells with a short hairpin RNA (shRNA) specific for MMP-14 (Mission Control shRNA from Sigma, code TRCN0000050855) as previously described (Llorente et al., 2020); a scrambled shRNA (code SHC005) was used to generate the control cell line (named as clone 8). The clone line showing the lowest expression of MMP-14 was selected for further studies (named as clone 3). Culture conditions for these cells were the same as for the SK-N-MC parental line, with the selection antibiotic present throughout their growth.

2.2. Cell treatments

2.2.1. HSV-1 infection conditions

The HSV-1 strain KOS 1.1 was obtained, propagated and titered on a monolayer of Vero cells following described methods (Carrascosa et al. 1982) and stored at –70 °C. SK-N-MC cells were seeded in complete media at 70–80% confluency and exposed to HSV-1 at 37 °C for 1 h (viral adsorption). In order to remove unbound virus, the medium was changed, and cells were incubated in complete medium at 37 °C. Multiplicity of infection (moi - expressed in plaque forming units per cell [pfu/cell]) used in all experiments was moi 1. The infected cells were analyzed at the hours post infection (hpi) indicated in each experiment. The infectious titers of HSV-1 were determined by plaque assays with Vero cells as previously described (Santana et al., 2012a, b).

2.2.2. Induction of oxidative stress

Mild oxidative stress was induced as previously described (Recuero et al., 2009) by adding xanthine (10 μ M; Sigma) and xanthine oxidase (50 mU/mL; Roche) (X-XOD) for 24 h. X-XOD was added after the virus adsorption and maintained until the end of infection.

2.2.3. Pharmacological inhibition of MMP-14

MMP-14 inhibition was performed by adding the cell permeating, selective inhibitor NS405020 (Remacle et al., 2012), at 100 μ M to the culture medium, unless otherwise indicated in specific experiments. NS405020 (APEX-BIO) was added after the virus adsorption and maintained until the end of infection, unless otherwise indicated. The effect of the inhibitor on cell viability was assessed by measuring the metabolic state of the cultures with an MTT assay as previously described (Recuero et al., 2009).

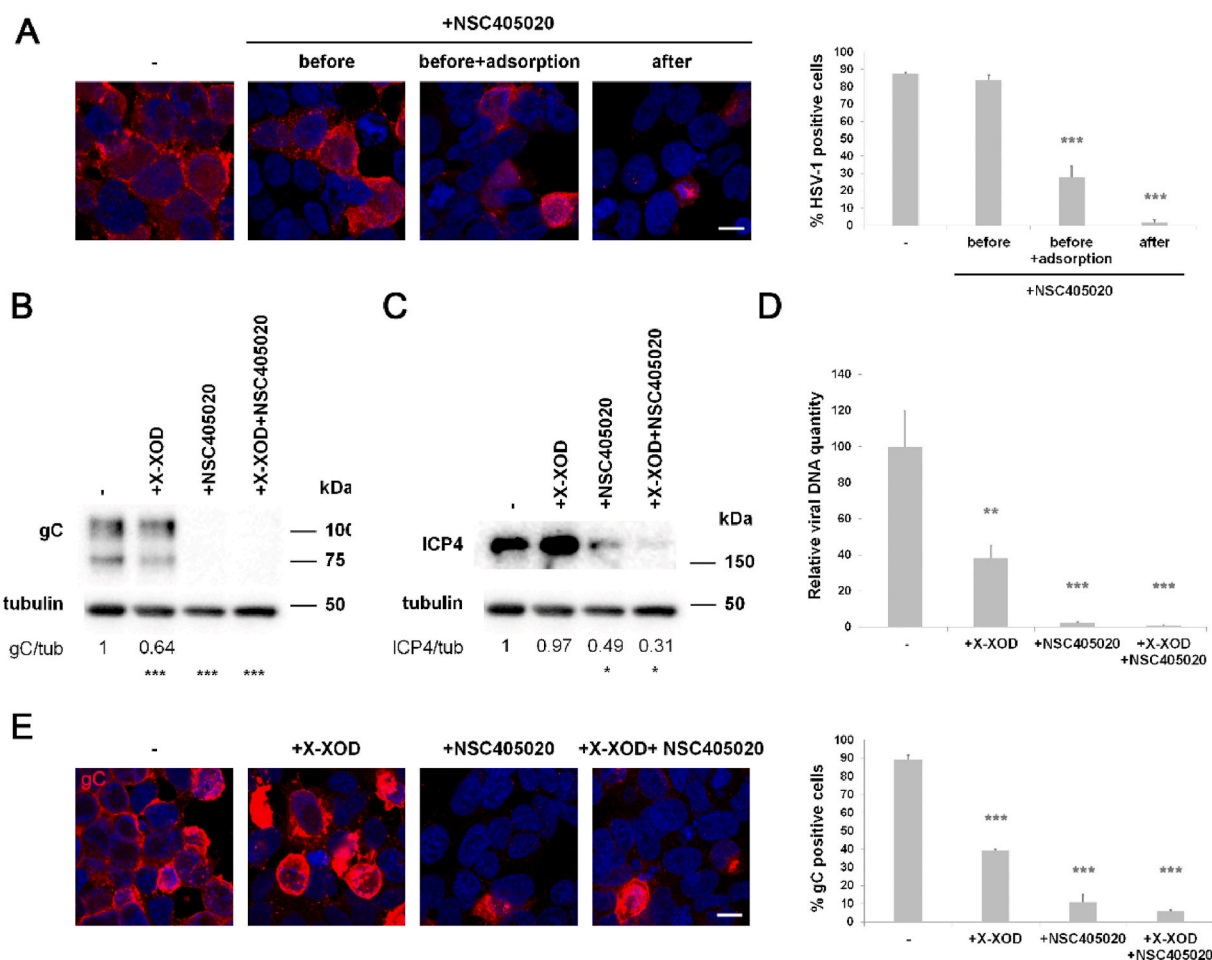


Fig. 1. MMP-14 inhibition reduces HSV-1 infection. A) SK-N-MC cells were infected with HSV-1 and treated with NSC405020. Cells were compared by confocal microscopy adding NSC405020 24 h before, including or not the time of adsorption, or after the HSV-1 adsorption. The representative panel show immunofluorescence images for anti-HSV-1 antibody and DAPI-stained nuclei. Original magnification: $63\times$. Scale bar: $10\mu\text{m}$. Quantification of infected cells by HSV-1 staining was performed and the graphs show the percentage of HSV-1-positive cells. At least 200 nuclei were counted from 2 independent experiments (minimum of 100 nuclei per experiment). Graphs depict the mean \pm SEM. B & C) SK-N-MC cells were infected with HSV-1 and treated with NSC405020 after the adsorption in the presence or absence of X-XOD for 24 h. Western blot was performed using anti-gC, anti-ICP4 and anti α -tubulin antibodies. Numbers represent the relative ratio of the densitometric value normalized against α -tubulin. * $p < 0.05$, ** $p < 0.01$ ($n = 4$ independent experiments). D) Viral DNA quantification was performed and represented as viral DNA copy numbers per ng of genomic DNA for each condition ($n = 3$ independent experiments). E) Cells were examined by confocal microscopy. The representative panel shows immunofluorescence images for anti-gC antibody and DAPI-stained nuclei. Original magnification $63\times$. Scale bar $10\mu\text{m}$. Quantification of infected cells by gC staining was performed and the graphs show the percentage of gC-positive cells. At least 450 nuclei were counted from 3 independent experiments (minimum of 150 nuclei per experiment). Graphs depict the mean \pm SEM.

2.3. Cell analysis

2.3.1. Viral DNA quantification by real-time quantitative polymerase chain reaction (qPCR)

The amount of HSV-1 DNA was quantified by real-time quantitative PCR. DNA was extracted using the QIAamp® DNA Mini Kit (QIAGEN) according to the manufacturer's instructions, as previously described (Santana et al., 2013). The concentration of viral DNA was then quantified by qPCR with an ABI Prism 7900HT SD® system (Applied Biosystems) using a custom designed TaqMan probe specific for the US12 viral gene (5'-AGGCGGCCAGAAC-3'). Viral DNA content was then normalized in terms of human genomic DNA, quantified with a pre-designed TaqMan probe specific for the 18S gene (Hs99999901_s1, Applied Biosystems). The quantification results were represented as viral DNA copy numbers per ng of genomic DNA.

2.3.2. Western blotting

Western blotting was performed on cell extracts as previously described (Llorente et al., 2018) with the primary antibodies listed in

Table 1 and horseradish peroxidase-coupled secondary antibodies. Immunodetection was performed using ECLTM Western Blotting Detection Reagents (GE Healthcare Life Sciences) according to the manufacturer's instructions. To quantify the intensity of the protein bands, densitometric analysis was performed using Quantity One® Software (Bio-Rad).

2.3.3. Immunofluorescence and immunocytochemistry

Immunofluorescence assays were performed as previously described (Recuerdo et al., 2010), employing the primary antibodies listed in Table 1 and Alexa Fluor-coupled secondary antibodies. Cells were examined using an LSM 710 laser scanning confocal microscope (Zeiss) coupled to a vertical M2 AxioImager (Zeiss) equipped with a 63X/1.4 Plan-Apochromat oil objective lens. Pictures were taken with a Spot RT digital camera (Diagnostic) using Zeiss ZEN 2010 imaging system software. Images were processed using Adobe Photoshop CS3.

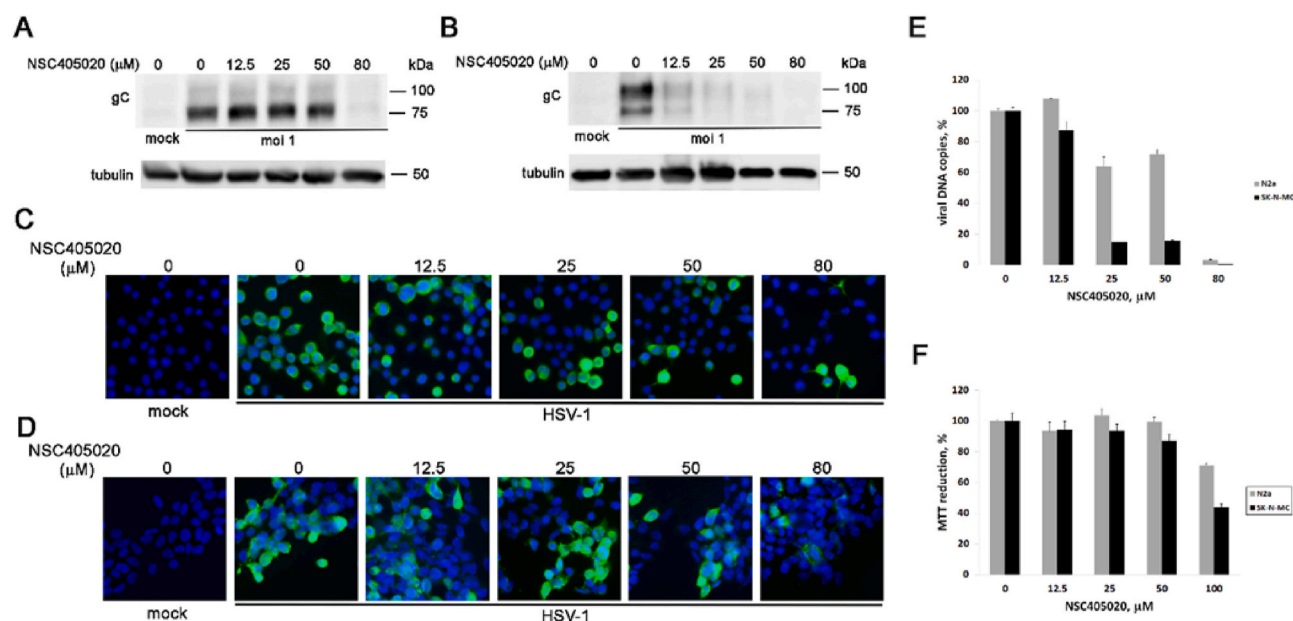


Fig. 2. NSC405020 inhibits HSV-1 infection of neuroblastoma cells in a dose-dependent manner. The human and murine cell lines SK-N-MC and N2a were infected with HSV-1 for 24 h in the absence or presence of different doses of NSC405020 added after viral adsorption. A & B) Western blot was performed using anti-gC and anti α -tubulin antibodies. A representative experiment is shown for the SK-N-MC (A) and N2a (B) cells. C & D) Cells were examined by fluorescence microscopy. The images show fluorescence of anti-gC antibody and DAPI-stained nuclei in SK-N-MC (C) and N2a (D) cells. Original magnification: $63 \times$. Scale bar: 10 μ m. E) Viral DNA quantification was performed by qPCR and represented as viral DNA copy numbers per ng of genomic DNA at the different doses of the inhibitor in the SK-N-MC (grey bars) and N2a (black bars) cells. Data are the mean with standard errors of two experiments. F) Cell injury induced by the inhibitor at different doses was measured in mock infected SK-N-MC (grey bars) and N2a (black bars) cells using the MTT reduction assay.

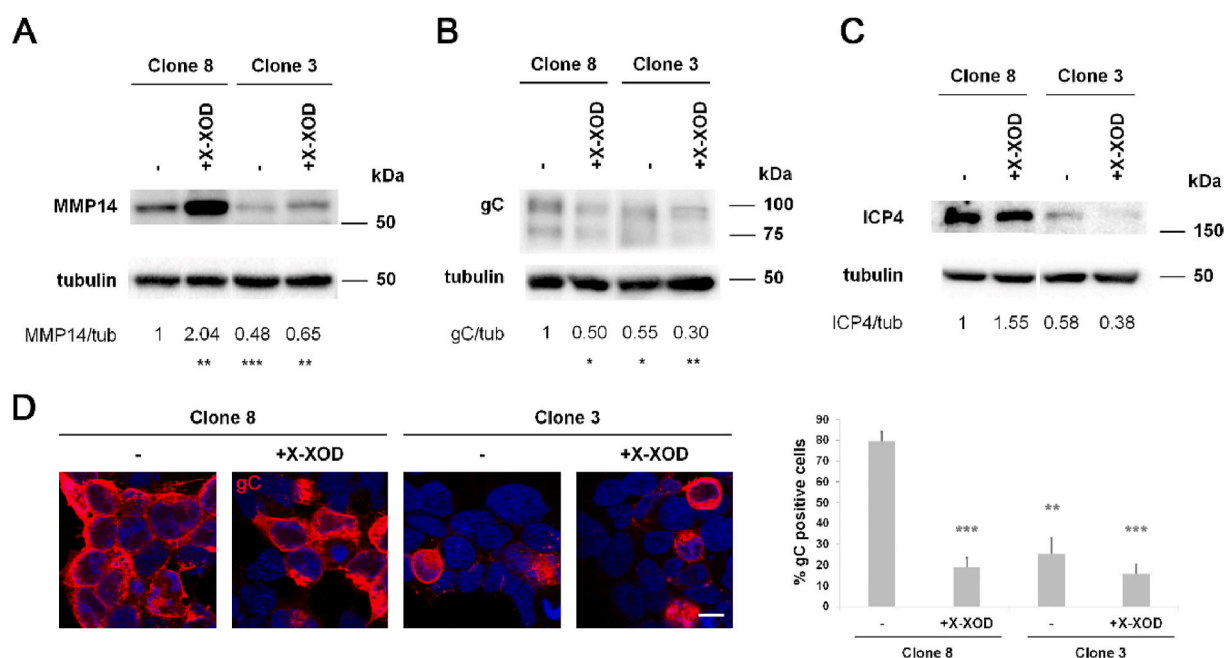


Fig. 3. MMP-14 deficiency reduces HSV-1 infection. MMP-14 deficient cells (clone 3) and control cells (clone 8) were infected with HSV-1 in the presence or absence of X-XOD for 24 h. A) Western blot was performed using anti-MMP14 and anti α -tubulin antibodies. Numbers represent the relative ratio of the densitometric value normalized against α -tubulin. $*p < 0.05$, $**p < 0.01$ ($n = 3$ independent experiments). B & C) Western blot was performed using anti-gC, anti-ICP4 and anti α -tubulin antibodies. Numbers represent the relative ratio of the densitometric value normalized against α -tubulin. $*p < 0.05$, $**p < 0.01$ ($n = 3$ independent experiments). D) Cells were examined by confocal microscopy. The representative panel shows immunofluorescence images for anti-gC antibody and DAPI-stained nuclei. Original magnification $63 \times$. Scale bar 10 μ m. Quantification of infected cells by gC staining was performed and the graphs show the percentage of gC-positive cells. At least 450 nuclei were counted from 3 independent experiments (minimum of 150 nuclei per experiment). Graphs depict the mean \pm SEM.

2.4. Statistical analysis

Values in graphs are expressed as mean \pm standard error of the mean

(SEM). Unless otherwise indicated in specific experiments, experimental groups were compared paired wise and the differences were analyzed using the one sample *t*-test. Significance was set at $p < 0.05$.

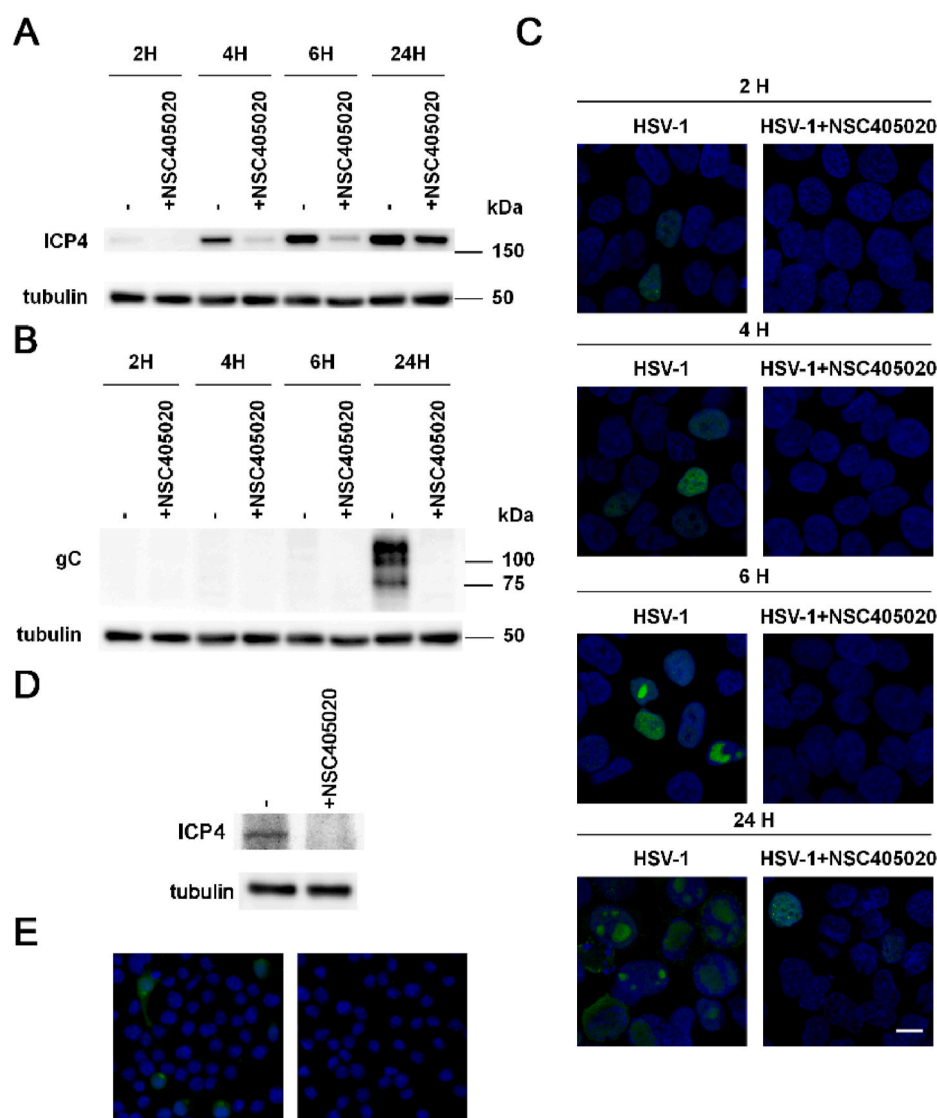


Fig. 4. MMP-14 inhibition affects early stages of HSV-1 infection. SK-N-MC (A–C) and N2a (D–E) cells were infected with HSV-1 and treated with NSC405020 for different times. A & B) Western blot was performed using anti-ICP4, anti-gC and anti α -tubulin antibodies. A representative experiment is shown. C) Cells were examined by confocal microscopy at the indicated times. The representative panel show immunofluorescence images for anti-ICP4 antibody and DAPI-stained nuclei. D) Western Blot and E) immunofluorescence images of N2a cells infected for 4 h in the absence or presence of NSC405020 with the anti-ICP4 antibody. Original magnification: $63 \times$. Scale bar: 10 μ m.

3. Results

3.1. MMP-14 inhibition or deficiency reduces HSV-1 infection

The involvement of MMP-14 on HSV-1 infection was assessed using the specific inhibitor NSC405020. SK-N-MC cells were treated with the inhibitor for 24 h before the infection, or the inhibitor was added after viral adsorption. Cells were examined by immunofluorescence with an anti-HSV-1 antibody at 24 h post infection (hpi). As shown in Fig. 1A, MMP-14 inhibition produced a clear decrease in the number of infected cells. Interestingly, the reduction was most prominent when the inhibitor was added after the viral adsorption, with less than 5% of the cells being HSV-1 positive, compared with the 85% of HSV-1 positive cells without the addition of the inhibitor. When the preincubation with the inhibitor was maintained during the viral adsorption the number of HSV-1 positive cells was a 30%, whereas the preincubation with the inhibitor had no effect in the percentage of HSV-1 positive cells. This result indicated that MMP-14 is involved in HSV-1 infection and suggests a role of this protein in viral post-entry steps. Taking these data into account, NSC405020 was added after HSV-1 adsorption in all the experiments.

To quantify the effect of MMP-14 inhibition, efficiency of HSV-1 infection was determined by assessing the levels of viral proteins and

DNA at 24 hpi. Since it has been described by our group that OS exacerbates the neurodegenerative markers induced by the virus (Santana et al., 2013) and that OS increases the levels of MMP-14 (Llorente et al., 2020), the infection was performed in the absence or presence of OS induced by the free radical-generating system X-XOD (Recuero et al., 2009).

Western blot analysis of SK-N-MC cell lysates were performed using antibodies specific for gC, that belongs to the class of $\gamma 2$ “true late” genes whose expression requires viral DNA synthesis, and ICP4, an immediate early protein whose expression begins before HSV-1 DNA replication. NSC405020 inhibitor induced a significant reduction, even to undetectable levels, of the gC and ICP4 amount both in the absence and presence of OS (Fig. 1B and C respectively). Consistent with these results, immunofluorescence analysis revealed that the cells treated with the inhibitor showed a marked decrease in the number of gC positive cells (approximately a 95%) (Fig. 1E), confirming the strong effect of the MMP-14 specific inhibitor NSC405020 on HSV-1 infection efficiency.

Similar results were observed when the viral DNA was quantified. A significant decrease -higher than 95%- of viral DNA copy number in the presence of NSC405020 was registered (Fig. 1D).

NSC405020 is widely reported as a repressor of tumor cell growth. For this reason, we next studied if the inhibition of HSV-1 infection could result from a decrease of cell viability. To this end, a dose curve of

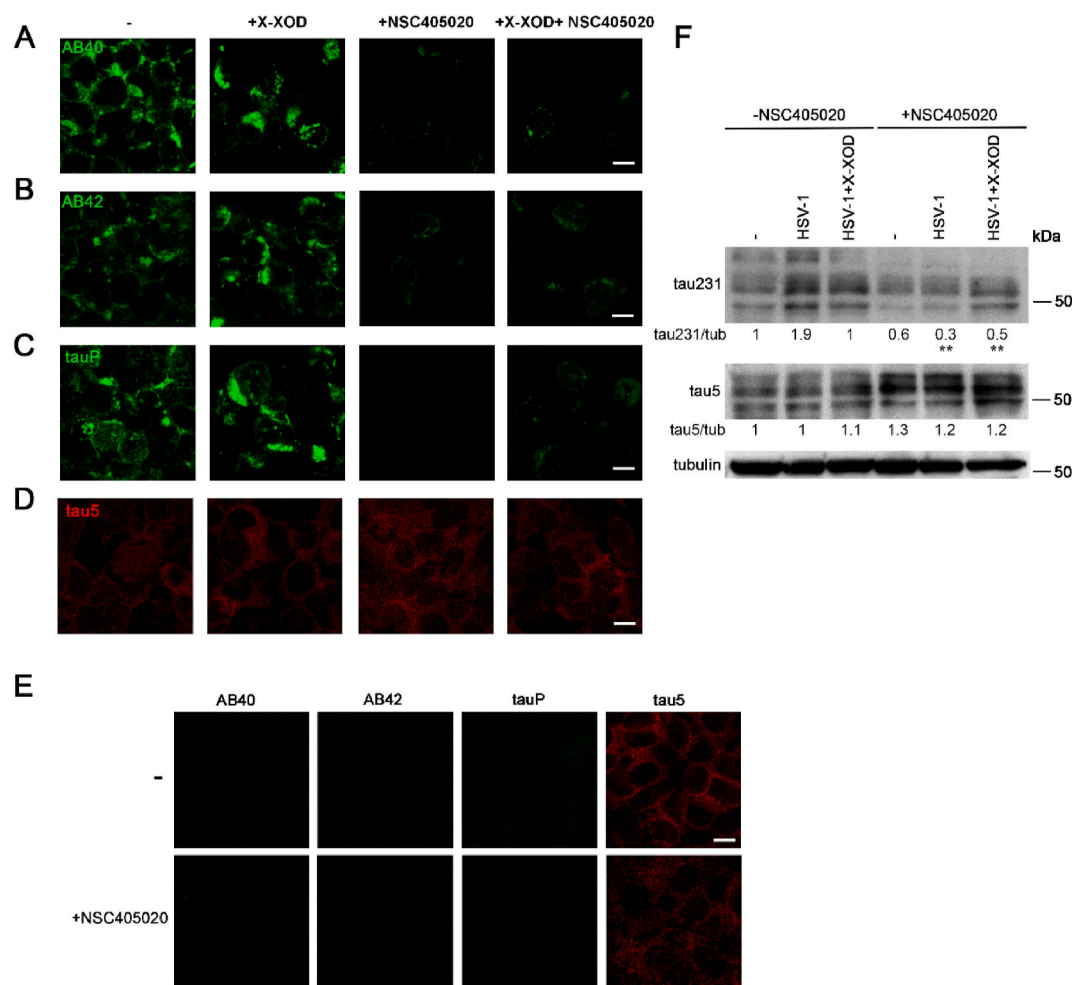


Fig. 5. MMP-14 inhibition reduces the accumulation of AD neurodegenerative markers induced by HSV-1. SK-N-MC cells were infected with HSV-1 and treated with NSC405020 in the presence or absence of X-XOD for 24 h and then were examined by confocal microscopy. The representative panel shows immunofluorescence images for anti-A β 40 (A), anti-A β 42 (B), anti-tauP (thr205) (C) and anti-total tau (tau5) (D) antibodies. Original magnification $63\times$. Scale bar 10 μ m. E) SK-N-MC mock infected cells were treated with NSC405020 for 24 h and examined by fluorescence microscopy with antibodies specific for the antigens indicated at the top. F) Western blot was performed using anti-tauP (thr231), tau5 and anti α -tubulin antibodies. Numbers represent the relative ratio of the densitometric value normalized against α -tubulin and referred to the value of the mock infected, untreated cells. * $p < 0.05$, ** $p < 0.01$ ($n = 3$ independent experiments).

the inhibitor was used, and the cell viability and infection efficiency was analyzed in SK-N-MC cells at 24 h post infection at the different doses. In addition, the murine neuroblastoma N2a cell line was used to validate the results in a different cell line. The results of this study are shown in Fig. 2. As shown in Fig. 2F, a moderate inhibition of MTT reduction was evidenced only at the highest concentration used (100 μ M). By contrast, a pronounced decrease in all the indicators of the efficiency of the infection, including the levels of gC protein (A and B), the number of infected cells (C and D) and the levels of viral DNA (E), was observed from an inhibitor dose of 25 μ M in both cell lines. According to the dose curves, slightly varying depending on the quantification measure used (viral DNA content, gC levels or percentage of infected cells), the IC₅₀ can be estimated between 12.5 and 25 μ M for SK-N-MC cells, and around 50 μ M for N2a cells. These experiments indicated that the effect of the inhibitor on HSV-1 infection was much higher than that attributable to an inhibition of cell growth or an increase in cell mortality.

To control for potential off-target effects of the drug, experiments in SK-N-MC cells stably expressing an MMP-14 specific shRNA were also carried out (Fig. 3). To check the efficiency of the gene silencing, MMP-14 levels were measured by Western blot (Fig. 3A). Viral protein levels and infected cell numbers were significantly lower in the MMP-14 deficient cells (clone 3), validating the data obtained with the inhibitor.

In sum, these results indicate that MMP-14 is involved in HSV-1

infection of human neuroepithelioma and murine neuroblastoma cells, since the number of infected cells and the amount of viral DNA, gC and ICP4 proteins are clearly decreased when MMP-14 is inhibited.

3.2. MMP-14 inhibition affects HSV-1 infection at early stages of the viral cycle

The strong effect of MMP-14 inhibitor after the viral adsorption step compared with that of cell pretreatment (Fig. 1) suggested that the main role of this protein in the viral infectious cycle is related with intracellular stages. The effect of MMP-14 on early stages of the viral cycle was assessed by quantifying the number of infected cells and the ICP4 levels by Western blot and immunofluorescence analysis. ICP4 is expressed at the very early stages of the infectious process, so infected cells were analyzed at early (2, 4, 6 hpi) and late times (24 hpi) post infection by Western blot (Fig. 4A). NSC405020 diminished the ICP4 levels at all times studied, indicating that MMP-14 plays a role in the first stages of infection, previous to DNA replication. As expected, the levels of gC were only detectable at late time (Fig. 4B), and the levels were also affected by the inhibitor as previously observed (Fig. 1B).

When cells were analyzed by immunofluorescence (Fig. 4C), ICP4 firstly showed a diffuse distribution in the nucleus, and later accumulated in small, dotted structures termed pre-replicative sites. As the

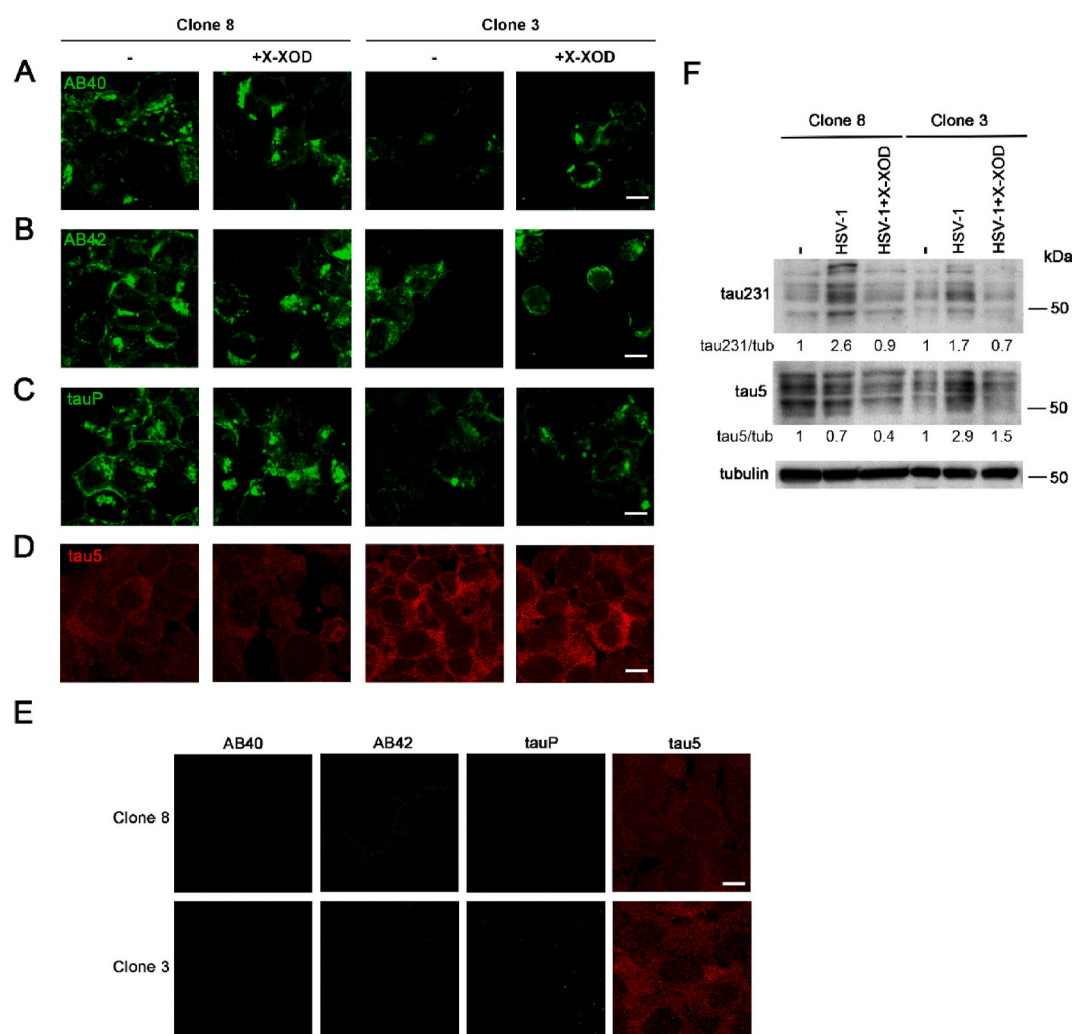


Fig. 6. MMP-14 deficiency reduces the accumulation of AD neurodegenerative markers induced by HSV-1. MMP-14 deficient cells (clone 3) and control cells (clone 8) were infected with HSV-1 in the presence or absence of X-XOD for 24 h and then were examined by confocal microscopy. The representative panel shows immunofluorescence images for anti-A β 40 (A), anti-A β 42 (B), anti-tauP (thr205) (C) and anti-tau5 (D) antibodies. E) Mock infected cells were treated with NSC405020 for 24 h and examined by fluorescence microscopy with antibodies specific for the antigens indicated at the top. Original magnification 63 \times . Scale bar 10 μ m. F) Western blot was performed using anti-tauP (thr231), tau5 and anti α -tubulin antibodies. Numbers represent the relative ratio of the densitometric value normalized against α -tubulin and referred to the value of the mock infected cells.

infection progressed, large globular viral replication compartments, were generated, where ICP4 was involved in the transcription and replication of viral DNA. NSC405020 inhibitor decreased the number of ICP4-positive cells at all times analyzed, consistently with the results obtained by Western blot. These findings confirm the effect of the MMP-14 inhibitor in early stages of HSV-1 infection cycle.

To validate these results, the levels of ICP4 were also measured in the N2a cell line. Results showed that the levels of ICP4 in Western Blot assays (Fig. 4D), and the number of cells stained with anti-ICP4 antibody (Fig. 4E) at 4 hpi were markedly reduced, indicating that the effect of NSC405020 in HSV-1 infection is not restricted to a unique cell line.

3.3. MMP-14 inhibition or deficiency reduces the accumulation of AD neurodegenerative markers induced by HSV-1

HSV-1 has been reported to induce neurodegenerative markers characteristic of AD, and these effects are exacerbated by OS (Santana et al., 2013). To analyze the role of MMP-14 on AD neurodegenerative markers induced by HSV-1, SK-N-MC cells infected with HSV-1 were treated with the inhibitor NSC405020, and the content of A β and phosphorylated tau were analyzed at 24 hpi in the absence or presence

of OS (Fig. 5).

First, A β levels were analyzed by immunofluorescence assays. The inhibitor NSC405020 caused a strong decrease of the accumulation of A β 40 and A β 42 (Fig. 5A and B respectively) in HSV-1 infected cells, both in the absence and presence of OS. The levels of phosphorylated tau were evaluated by immunofluorescence and Western blot analysis, using antibodies that recognize phosphorylated epitopes present in AD brains (thr 205 and thr 231), and the tau 5 antibody that recognizes phosphorylated and non-phosphorylated forms of tau. Immunofluorescence analysis revealed a strong decrease of phosphorylated tau staining (Fig. 5C) in the cells treated with NSC405020, whereas total tau seemed to increase in the presence of the inhibitor (Fig. 5D). Moreover, when phosphorylated and total tau levels were analyzed by Western blot, a significant decrease of phosphorylated tau (Fig. 5E) and a trend of increase in total tau (Fig. 5F) was observed in the presence of the inhibitor NSC405020, confirming the results obtained in the immunofluorescence studies.

As in the HSV-1 infection assays, AD neurodegenerative marker analyses were also performed in MMP-14 silenced cells to ensure there were no side effects caused by the drug (Fig. 6). The accumulation of A β and phosphorylated tau decreased in MMP-14 deficient cells (clone 3) in

the absence or presence of OS, validating the data obtained with the inhibitor. Moreover, when phosphorylated and total tau levels were analyzed by Western blot, a relative decrease of phosphorylated tau and an increase in total tau (Fig. 6F) was observed in the HSV-1 infected deficient cells (clone 3) in comparison with the control (clone 8), what reinforced the results obtained in the immunofluorescence studies.

In sum, these results indicate that the impairment of HSV-1 infection produced by the inhibition or deficiency of MMP-14 affects AD neurodegenerative events induced by the virus.

There are previous reports showing MMP-14 as a relevant player in the inflammatory response raised by viral infections, and in the dissemination of viruses through its role as a protease degrading extracellular matrix components (Jobin et al. 2017; Young et al., 2019). However, this is, to our knowledge, the first report showing the direct implication of MMP-14 in HSV-1 infectious cycle, since its inhibition significantly reduced the efficiency of HSV-1 infection. Further, MMP-14 inhibition also significantly reduced the AD neurodegenerative events associated to HSV-1 infection, the accumulation of A β and phosphorylated tau.

More studies are needed to reveal the mechanisms by which MMP-14 interferes with HSV 1 infectious cycle. However, it is widely reported that viruses utilize endocytosis as the most common entry pathway. After binding to the cellular surface, the various endocytic pathways allow viruses to ferry their capsids through the cytoplasm where cortical actin filaments and other cytoplasmic barriers are overcome to reach the nucleus. The envelope of HSV-1 can either fuse with the plasma membrane or with vesicle membranes after virions are internalized via endocytosis (Nicola 2016). Since MMP-14 is implicated in the lysosomal system, as previously described by our group (Llorente et al., 2020), the inhibition of MMP-14 may impair the endocytic internalization and dispersion of the virus within the cell. From the experiments performed in this work, we can conclude that MMP-14 inhibition affects early intracellular stages of the viral cycle of HSV-1, significantly inhibiting the expression of the immediate early protein ICP4. However, given the wide array of potential target proteins and pathways regulated by MMP-14 in the cell (Jobin et al. 2017), it cannot be excluded that additional steps of the viral cycle depending on these pathways are also inhibited. The use of irreversible inhibitors of the protease would be a valuable tool to this aim; given the renewed interest of MMP-14 as a pharmaceutical target (Fields 2019), these further studies are guaranteed.

Our data have demonstrated that MMP-14 inhibition has a strong effect on HSV-1 infection and the consequent induction of neurodegenerative markers characteristic of AD brains. MMP-14 therefore has the potential to be a target to develop novel antiviral treatments, which has been previously claimed to reduce the development of dementia (Tzeng et al., 2018). In addition, the direct role of MMP-14 in APP proteolysis, recently reported by our group and others (Llorente et al., 2020) (Paumier et al., 2019), raises the possibility that targeting MMP-14 could have an additional effect specifically targeting the upregulation of the amyloidogenic pathway induced by HSV-1. In this way, MMP-14 could be a good antiviral target that, in comparison with already known treatments, could pose additional specificity towards the neurodegenerative effects associated with the infection. In conclusion, the inhibition of MMP-14 may be particularly suitable for further experimental testing to develop treatment protocols for patients showing neurodegeneration as a consequence of HSV-1 infection, such as AD patients, with the aim of slowing or stopping disease progression.

Funding

This work was supported by the Ministerio de Ciencia, Innovación y Universidades (SAF2017-85747-R).

Research data

Data available on request. María J Bullido should be contacted to request the data.

Declaration of competing interest

The authors declare that they have no known competing financial interests or personal relationships that could have appeared to influence the work reported in this paper.

Acknowledgment

The institutional grants of Fundación Ramón Areces and Banco de Santander to the Centro de Biología Molecular Severo Ochoa are gratefully acknowledged.

References

- Alvarez, G., Aldudo, J., Alonso, M., Santana, S., Valdivieso, F., 2012. 'Herpes simplex virus type 1 induces nuclear accumulation of hyperphosphorylated tau in neuronal cells'. *J. Neurosci. Res.* 90, 1020–1029.
- Carrascosa, A.L., Santaren, J.F., Vinuela, E., 1982. 'Production and titration of African swine fever virus in porcine alveolar macrophages. *J. Virol Methods* 3, 303–310.
- Eimer, W.A., Vijaya Kumar, D.K., Navalpur Shanmugam, N.K., Rodriguez, A.S., Mitchell, T., Washicosky, K.J., Gyorgy, B., Breakefield, X.O., Tanzi, R.E., Moir, R.D., 2018. 'Alzheimer's disease-associated beta-amyloid is rapidly seeded by Herpesviridae to protect against brain infection. *Neuron* 99, 56–63 e3.
- Elkington, P.T., O'Kane, C.M., Friedland, J.S., 2005. 'The paradox of matrix metalloproteinases in infectious disease. *Clin. Exp. Immunol.* 142, 12–20.
- Fields, G.B., 2019. The rebirth of matrix metalloproteinase inhibitors: moving beyond the dogma. *Cells* 8, 984–1008.
- Fulop, T., Itzhaki, R.F., Balin, B.J., Miklosy, J., Barron, A.E., 2018. Role of microbes in the development of alzheimer's disease: state of the art - an international symposium presented at the 2017 IAGG congress in san francisco'. *Front. Genet.* 9, 362.
- Haas, J.G., Lathe, R., 2018. Microbes and alzheimer's disease: new findings call for a paradigm change. *Trends Neurosci.* 41, 570–573.
- Harris, S.A., Harris, E.A., 2015. 'Herpes simplex virus type 1 and other pathogens are key causative factors in sporadic alzheimer's disease. *J. Alzheimers Dis* 48, 319–353.
- Harris, S.A., Harris, E.A., 2018. 'Molecular mechanisms for herpes simplex virus type 1 pathogenesis in alzheimer's disease. *Front. Aging Neurosci.* 10, 48.
- Itzhaki, R.F., 2016. 'Herpes and alzheimer's disease: subversion in the central nervous system and how it might be halted. *J. Alzheimers Dis* 54, 1273–1281.
- Itzhaki, R.F., 2018. 'Corroboration of a major role for herpes simplex virus type 1 in alzheimer's disease. *Front. Aging Neurosci.* 10, 324.
- Itzhaki, R.F., Cosby, S.L., Wozniak, M.A., 2008. 'Herpes simplex virus type 1 and Alzheimer's disease: the autophagy connection. *J. Neurovirol.* 14, 1–4.
- Itzhaki, R.F., Lin, W.R., Shang, D., Wilcock, G.K., Faragher, B., Jamieson, G.A., 1997. 'Herpes simplex virus type 1 in brain and risk of Alzheimer's disease. *Lancet* 349, 241–244.
- Jamieson, G.A., Maitland, N.J., Wilcock, G.K., Craske, J., Itzhaki, R.F., 1991. 'Latent herpes simplex virus type 1 in normal and Alzheimer's disease brains. *J. Med. Virol.* 33, 224–227.
- Jobin, P.G., Butler, G.S., Overall, C.M., 2017. 'New intracellular activities of matrix metalloproteinases shine in the moonlight. *Biochim. Biophys. Acta Mol. Cell Res.* 1864, 2043–2055.
- Kristen, H., Sastre, I., Munoz-Galdeano, T., Recuero, M., Aldudo, J., Bullido, M.J., 2018. 'The lysosome system is severely impaired in a cellular model of neurodegeneration induced by HSV-1 and oxidative stress. *Neurobiol. Aging* 68, 5–17.
- Letenneur, L., Peres, K., Fleury, H., Garrigue, I., Barberger-Gateau, P., Helmer, C., Orgogozo, J.M., Gauthier, S., Dartigues, J.F., 2008. 'Seropositivity to herpes simplex virus antibodies and risk of Alzheimer's disease: a population-based cohort study. *PLoS One* 3, e3637.
- Llorente, P., Kristen, H., Sastre, I., Toledano-Zaragoza, A., Aldudo, J., Recuero, M., Bullido, M.J., 2018. 'A free radical-generating system regulates amyloid oligomers: involvement of cathepsin B. *J. Alzheimers Dis* 66, 1397–1408.
- Llorente, P., Martins, S., Sastre, I., Aldudo, J., Recuero, M., Adjaye, J., Bullido, M.J., 2020. 'Matrix metalloproteinase 14 mediates APP proteolysis and lysosomal alterations induced by oxidative stress in human neuronal cells. *Oxid Med Cell Longev* 16, 5917187.
- Lovheim, H., Gilthorpe, J., Adolfsson, R., Nilsson, L.G., Elgh, F., 2015. 'Reactivated herpes simplex infection increases the risk of Alzheimer's disease. *Alzheimers Dement* 11, 593–599.
- Martinez-Torres, F.J., Wagner, S., Haas, J., Kehm, R., Sellner, J., Hacke, W., Meyding-Lamade, U., 2004. 'Increased presence of matrix metalloproteinases 2 and 9 in short- and long-term experimental herpes simplex virus encephalitis. *Neurosci. Lett.* 368, 274–278.
- Nicola, A.V., 2016. 'Herpesvirus entry into host cells mediated by endosomal low pH. *Traffic* 17, 965–975.

- Paumier, J.M., Py, N.A., Garcia-Gonzalez, L., Bernard, A., Stephan, D., Louis, L., Checler, F., Khrestchatsky, M., Baranger, K., Rivera, S., 2019. 'Proamyloidogenic effects of membrane type 1 matrix metalloproteinase involve MMP-2 and BACE-1 activities, and the modulation of APP trafficking. *FASEB J.* 33, 2910–2927.
- Readhead, B., Haure-Mirande, J.V., Funk, C.C., Richards, M.A., Shannon, P., Haroutunian, V., Sano, M., Liang, W.S., Beckmann, N.D., Price, N.D., Reiman, E.M., Schadt, E.E., Ehrlich, M.E., Gandy, S., Dudley, J.T., 2018. Multiscale Analysis of independent alzheimer's cohorts finds disruption of molecular, genetic, and clinical networks by human herpesvirus. *Neuron* 99, 64–82 e7.
- Recuero, M., Munoz, T., Aldudo, J., Subias, M., Bullido, M.J., Valdivieso, F., 2010. A free radical-generating system regulates APP metabolism/processing. *FEBS Lett.* 584, 4611–4618.
- Recuero, M., Vicente, M.C., Martinez-Garcia, A., Ramos, M.C., Carmona-Saez, P., Sastre, I., Aldudo, J., Vilella, E., Frank, A., Bullido, M.J., Valdivieso, F., 2009. 'A free radical-generating system induces the cholesterol biosynthesis pathway: a role in Alzheimer's disease. *Aging Cell* 8, 128–139.
- Remacle, A.G., Golubkov, V.S., Shiryaev, S.A., Dahl, R., Stebbins, J.L., Chernov, A.V., Cheltsov, A.V., Pellecchia, M., Strongin, A.Y., 2012. 'Novel MT1-MMP small-molecule inhibitors based on insights into hemopexin domain function in tumor growth. *Canc. Res.* 72, 2339–2349.
- Rojas-Quintero, J., Wang, X., Tipper, J., Burkett, P.R., Zuniga, J., Ashtekar, A.R., Polverino, F., Rout, A., Yambayev, I., Hernandez, C., Jimenez, L., Ramirez, G., Harrod, K.S., Owen, C.A., 2018. 'Matrix metalloproteinase-9 deficiency protects mice from severe influenza A viral infection. *JCI Insight* 3.
- Santana, S., Bullido, M.J., Recuero, M., Valdivieso, F., Aldudo, J., 2012a. 'Herpes simplex virus type I induces an incomplete autophagic response in human neuroblastoma cells'. *J. Alzheimers Dis* 30, 815–831.
- Santana, S., Recuero, M., Bullido, M.J., Valdivieso, F., Aldudo, J., 2012b. 'Herpes simplex virus type I induces the accumulation of intracellular beta-amyloid in autophagic compartments and the inhibition of the non-amyloidogenic pathway in human neuroblastoma cells. *Neurobiol. Aging* 33, 430 e19–33.
- Santana, S., Sastre, I., Recuero, M., Bullido, M.J., Aldudo, J., 2013. 'Oxidative stress enhances neurodegeneration markers induced by herpes simplex virus type 1 infection in human neuroblastoma cells. *PLoS One* 8 e75842.
- Sufiawati, I., Tugizov, S.M., 2018. 'HIV-induced matrix metalloproteinase-9 activation through mitogen-activated protein kinase signalling promotes HSV-1 cell-to-cell spread in oral epithelial cells. *J. Gen. Virol.* 99, 937–947.
- Talmi-Frank, D., Altboum, Z., Solomonov, I., Udi, Y., Jaitin, D.A., Klepfish, M., David, E., Zhuravlev, A., Keren-Shaul, H., Winter, D.R., Gat-Viks, I., Mandelboim, M., Ziv, T., Amit, I., Sagi, I., 2016. Extracellular matrix proteolysis by MT1-MMP contributes to influenza-related tissue damage and mortality. *Cell Host Microbe* 20, 458–470.
- Tzeng, N.S., Chung, C.H., Lin, F.H., Chiang, C.P., Yeh, C.B., Huang, S.Y., Lu, R.B., Chang, H.A., Kao, Y.C., Yeh, H.W., Chiang, W.S., Chou, Y.C., Tsao, C.H., Wu, Y.F., Chien, W.C., 2018. 'Anti-herpetic medications and reduced risk of dementia in patients with herpes simplex virus infections-a nationwide, population-based cohort study in taiwan. *Neurotherapeutics* 15, 417–429.
- Wozniak, M.A., Itzhaki, R.F., Shipley, S.J., Dobson, C.B., 2007. 'Herpes simplex virus infection causes cellular beta-amyloid accumulation and secretase upregulation. *Neurosci. Lett.* 429, 95–100.
- Wozniak, M.A., Mee, A.P., Itzhaki, R.F., 2009. 'Herpes simplex virus type 1 DNA is located within Alzheimer's disease amyloid plaques. *J. Pathol.* 217, 131–138.
- Young, D., Das, N., Anowai, A., Dufour, A., 2019. 'Matrix metalloproteases as influencers of the cells' social media. *Int. J. Mol. Sci.* 20.